Surface Potentials Measure Ion Concentrations near Lipid Bilayers during Rapid Solution Changes

Derek R. Laver* and Brian A. Curtis#

*Muscle Research Group, Division of Neuroscience, John Curtin School of Medical Research, Australian National University, Canberra ACT 2601, Australia, and #University of Illinois College of Medicine at Peoria, Peoria, Illinois 61656 USA

ABSTRACT We describe a puffing method for changing solutions near one surface of lipid bilayers that allows simultaneous measurement of channel activity and extent of solution change at the bilayer surface. Ion adsorption to the lipid headgroups and screening of the bilayer surface charge by mobile ions provided a convenient probe for the ionic composition of the solution at the bilayer surface. Rapid ionic changes induced a shift in bilayer surface potential that generated a capacitive transient current under voltage-clamp conditions. This depended on the ion species and bilayer composition and was accurately described by the Stern-Gouy-Chapman theory. The time course of solute concentrations during solution changes could also be modeled by an exponential exchange of bath and puffing solutions with time constants ranging from 20 to 110 ms depending on the flow pressure. During changes in $[Cs^+]$ and $[Ca^{2+}]$ (applied separately or together) both the mixing model and capacitive currents predicted $[Cs^+]$ and $[Ca^{2+}]$ transients consistent with those determined experimentally from: 1) the known Cs^+-dependent conductance of open ryanodine receptor channels and 2) the Ca^{2+}-dependent gating of ryanodine receptor Ca^{2+} channels from cardiac and skeletal muscle.

INTRODUCTION

Planar artificial lipid bilayers are commonly used to study the function of membrane transport proteins including ion channels. The bilayer technique provides a convenient way of measuring current flow through individual ion channels that normally reside in membranes that are not accessible by the patch-clamp method. Most studies of single channels concentrate on the properties that ion channels display under stationary conditions. As ion channels in vivo often function in response to rapidly varying concentrations of regulatory ligands and to changes in membrane potential it is physiologically more relevant to study their nonstationary properties. To this end, some recent bilayer studies (e.g., Gyorke and Fill, 1994a; Valdivia et al., 1995; Sitsapesan et al., 1995b; Laver and Curtis, 1996) measured the response of ryanodine receptor Ca^{2+} release channels (RyRs) to rapid changes in $[Ca^{2+}]$ that are likely to occur in muscle.

Sitsapesan et al. (1995a) have achieved solution changes on the order of 10 ms by forming a bilayer at the tip of a pipette and rapidly moving that pipette from one solution stream to another. Much faster $[Ca^{2+}]$ rise times on the order of 1 ms have been accomplished with flash-induced release of caged Ca^{2+} (Gyorke and Fill, 1994a; Valdivia et al., 1995). The conclusions drawn by these studies pivot on the exact form of the $[Ca^{2+}]$ time course, which has been the focus of some debate (Lamb et al., 1994; Gyorke and Fill, 1994b). This controversy highlights the need to know the time course of the solution composition near the bilayer during rapid changes.

The formation of liquid junction potentials at solution interfaces has been used to establish the timing of solution changes (Sitsapesan et al., 1995a), but these generally reveal little about the solute concentrations near the membrane during the change. Fast-responding Ca^{2+} indicators have been used to track the $[Ca^{2+}]$ transients produced by flash photolysis (Escobar et al., 1995). However, this method is applicable only when there exists suitable indicators of solute concentration.

We describe two methods for inferring changes in solute concentrations (solution transients) at a bilayer surface during solution changes that also allow simultaneous measurement of single-channel activity. 1) Solution changes induce a shift in bilayer surface potential that generate a transient, capacitive current through the bilayer under voltage-clamp conditions. 2) Solute concentrations during solution exchange appeared to follow an exponential time course that formed the basis for modeling solution transients. We show that quantitative estimates of solute concentrations can be derived using both methods.

MATERIALS AND METHODS

Materials

We are grateful to Dr. Pauline Junankar and Ms. Lin Roden for providing sarcoplasmic reticulum (SR) vesicles containing cardiac and skeletal isoforms of the RyRs. Skeletal SR vesicles were prepared from either the back or leg muscle of New Zealand rabbits, and cardiac vesicles were prepared from sheep hearts (Laver et al., 1995). Bilayers separating two aqueous baths (*cis* and *trans*) were formed from a mixture of palmitoyl-oleoyl-phosphatidylethanolamine (PE), palmitoyl-oleoyl-phosphatidylserine (PS) and palmitoyl-oleoyl-phosphatidylcholine (PE:PS:PC = 5:3:2, by weight) in *n*-decane using the film drainage technique of Mueller et al. (1962). Lipids were obtained in chloroform from Avanti Polar Lipids (Alabaster,

Received for publication 8 November 1995 and in final form 23 May 1996.

Address reprint requests to Dr. Derek R. Laver, Muscle Research Group, Division of Neuroscience, John Curtin School of Medical Research, Australian National University, GPO Box 334, Canberra, ACT 2601, Australia. Fax: 061-6-249-4761; E-mail: derek.laver@anu.edu.au.

0006-3495/96/08/722/10 $2.00

AL). SR vesicles were added to the *cis* bath, and when they fused with the bilayer, the myoplasmic side of the SR membrane (the ryanodine receptor) faced the *cis* solution. The method for incorporating ion channels is described by Laver et al. (1995). Unless otherwise stated, 10 mM TES was used to buffer pH and BAPTA was used to buffer pCa. Solutions were adjusted to pH 7.4 with CsOH and to a range of pCa with $CaCl_2$. Free $[Ca^{2+}]$ was measured using an ion meter (Radiometer ION83). The calibration of the ion meter was routinely checked by comparing its estimates of free $[Ca^{2+}]$ with theoretical estimates derived from the algorithm incorporated in the program COMICS (Perrin and Sayce, 1967) using standard reaction constants (Tsien, 1980).

Bilayer and solution exchange apparatus

Bilayers were formed across an aperture of 80 μm, and thinning of the lipid film to a bilayer was monitored visually with ×20 magnification and electrically by measurements of bilayer capacitance. The bilayer chamber was a 1.5-ml delrin cup that separated the two bathing solutions (*cis* and *trans*). Rapid exchange of solutions at the *cis* face of the bilayer was achieved by puffing solutions from a 0.5-mm ID stainless steel tube that was introduced into the myoplasmic chamber (Fig. 1). Using a micromanipulator, the tube was positioned as close as possible to the bilayer. The *trans* cup had a great deal of the lateral wall around the bilayer aperture machined away to provide adequate access for the puffing tube and flow solution. The beveled end of the puffing tube half covered the bilayer aperture from above and was ~50 μm in front of the bilayer. A spring-loaded clamp fitted with a microswitch was placed on the flexible tubing that connected a reservoir to the stainless steel tube. The switch allowed a capacitor discharge to be recorded on the second channel (normally voltage) of the recording system to mark the beginning of flow. Solution flow through the nozzle was proportional to the height of the reservoir above the bath up to 50 cm. The flow rates were usually in the range 0.4–0.8 $\mu l\ s^{-1}$ $(cm_{H_2O})^{-1}$ depending on the dimensions of the tubing and the viscosity of the puffing solution. A reservoir height of 5 cm allowed moderate rates of solution exchange while conserving bilayer integrity whereas heights greater than 15 cm were used to achieve rapid solution changes. Applications of flow solutions lasted several seconds and the solution was returned to normal, after shutting the flow valve, by stirring the bath for ~15 s. Gradual perfusion of the *cis* bath was done occasionally to prevent contamination of the *cis* bath by the flow solution. This was done using a back-to-back syringe system configured such that bath perfusion and waste withdrawal could be maintained at equal rates.

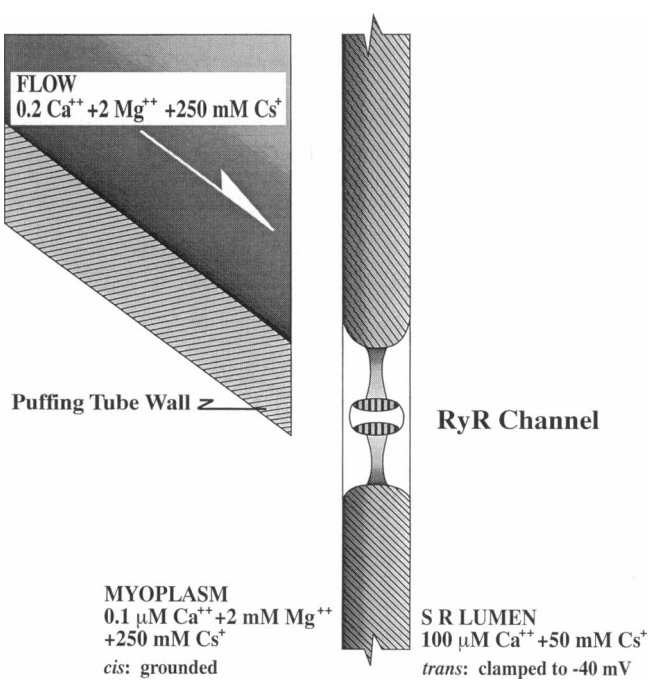

FIGURE 1 A schematic diagram of the flow tube and bilayer/channel. Exchange of solutions at the *cis* face of the bilayer was achieved by squirting solutions from a stainless steel tube (0.5 mm ID) positioned ~50 μm to the front of the bilayer, as close as practical. The relatively open access of the bilayer aperture to the *cis* bath facilitated rapid solution exchange near the bilayer.

Electrical connection with the bath was made using silver-chloride-coated silver wire immersed in an agar salt-bridge (containing 50 to 250 mM CsCl). The *cis* chamber was electrically grounded via the agar salt-bridge to prevent the tubing leading to the flow nozzle, the reservoir, and the solution they contained from becoming a source of electrical interference; the opposite of the usual convention. To retain convention in channel recordings, the bilayer potential difference is defined with respect to the *trans* chamber as ground and positive current as directed from the *cis* to *trans* bath. All measurements were carried out within the temperature range 23–26°C.

Data acquisition and analysis

Voltage was controlled and current recorded with an Axopatch 200A amplifier (Axon Instruments). During the experiments the bilayer current and potential were recorded at a bandwidth of 5 kHz on video tape using pulse code modulation (model 200; A. R. Vetter Co.). Before analysis, the flow indicator and current signals and were replayed through a 1-kHz, low-pass, 8-pole Bessel filter and sampled at 2 kHz per channel with a TL-1 DMA interface (Tecmar). These recordings were displayed and analyzed using an in-house program (Channel2, developed by Professor P. W. Gage and Mr. M. Smith). Episodes from the channel recordings were edited in synchrony with the flow indicator pulses, which were averaged to produce an ensemble channel response to rapid solution changes.

Capacitance measurements (~5% precision using a two-terminal method) were made by measuring the amplitude of the rectangular current response to voltage ramps (1 V/s) from −40 to +100 mV. Background capacitance attributable to the delrin cup was measured from the capacitance of the cup when the bilayer hole was occluded by a thick lipid/*n*-decane film. Bilayer capacitance (~200 pF) was calculated by subtracting the background capacitance (~50 pF) of the thick lipid/*n*-decane film from the total capacitance (~250 pF) once the bilayer had formed.

RESULTS

Analysis of bilayer current during solution exchange

Upon opening the valve in the tubing leading to the nozzle, the solution quickly established a steady sheath around the bilayer and neighboring septum. When the bath and puffing solutions had different refractive indices, observation (×20) of the puffing tube and bilayer revealed a single solution interface descending over the bilayer, as a curtain falling. The descent was rapid but clearly visible and the liquid interface showed no sign of turbulence. Two time delays intervened between opening the flow valve and complete exchange of solution at the bilayer/channel; namely, a flow delay and a mixing/diffusion delay. Both could be determined from the transient current (Fig. 2) generated by changing the solution against the bilayer. The transient began ~50 ms after the valve opened (flow delay), and the time when the current trace departed from the steady base-

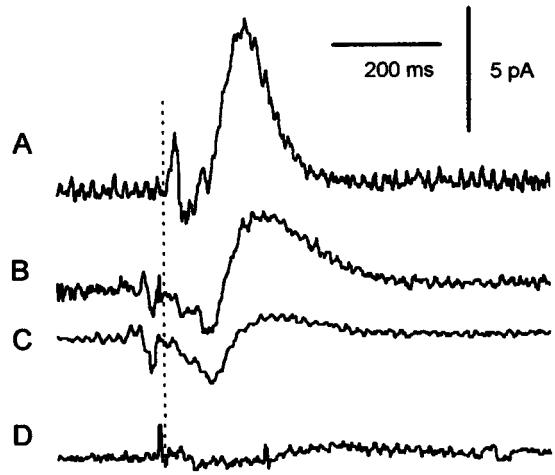

FIGURE 2 Individual current transients induced by changing $[Ca^{2+}]$, monovalent ion species, or [mannitol] in the *cis* bath. Records are filtered at 100 Hz. The solution exchange begins at 200 ms after the beginning of each trace (*vertical dashed line*). The bath solution (beginning of each trace) is replaced by the puffing solution during the transient. (*A*) (D14002) $[Ca^{2+}]$ decreased from 1 mM to 0.1 μM while [CsCl] remained at 250 mM. (*B*) (D13113) 250 mM NaCl plus 0.1 mM $CaCl_2$ replaced 250 mM CsCl plus 0.1 mM $CaCl_2$. (*C*) The same record as in *B* except that the flow valve was opened before the 250 mM NaCl from the previous puff had a chance to dilute into the 250 mM CsCl of the *cis* bath. Thus, the composition of the flow solution was nearly the same as that near the bilayer. The current response is believed to result from flow-induced distortion of the bilayer. (*D*) (D13111) 250 mM CsCl plus 500 mM mannitol replaced 250 mM CsCl.

line level was the first evidence of new solution coming in contact with the bilayer (see below). We suspect flow began gradually as the flexible tubing regained its circular cross section when the flow valve (pinch clamp) was released.

The transient current appeared to have two components. One depended on the ionic changes in the bath (i.e., changes in $[Cs^+]$, $[Mg^{2+}]$, and $[Ca^{2+}]$; see Fig. 2 *A* and *B*); it was proportional to the bilayer capacitance (not shown) and depended on the lipid composition of the bilayers. This component of the current transient was also sensitive to the exchange of ion species at constant ionic strength (Na^+ for Cs^+; Fig. 2 *B*) indicating that it arose from ion-specific as well as ionic-strength-dependent mechanisms. Apart from relatively small microphonic effects, the current transient was not present during changes in osmolality alone (Fig. 2 *D*; see below). The other component of the current transient depended on solution flow and was sometimes seen when the flow and bath solutions were identical (Fig. 2 *C*). This is probably an acoustic current driven by changes in bilayer capacitance resulting from flow-induced distortion of the bilayer during a puff. The brief spikes near the onset of solution exchange in Fig. 2 *A* also probably arise from acoustic effects. The size of the acoustic current could be measured directly by opening the flow valve within a second of the preceding puff. This protocol produced solution flow without significant change in the solution composition near the bilayer because the solution from the previous puff had insufficient time to dilute into the *cis* bath (Fig. 2 *C*).

Our findings suggest that the ion-dependent current transients result from a change in the surface potential on the side of the bilayer facing the nozzle. An asymmetric change in bilayer surface potential shifts the bilayer potential relative to the voltage-clamp potential (MacDonald and Bangham, 1972; McLaughlin, 1977), which drives a capacitive current through the bilayer and voltage-clamp system. This interpretation of the current transients is further supported by the quantitative analysis described below (Eqs. 1–3). The shift in bilayer potential, ΔV, can be calculated at any time t during the baseline transient by Eq. 1:

$$\Delta V = \frac{1}{C}\int_0^t I.dt \tag{1}$$

where I is the capacitive (ion-dependent) current and C is the bilayer capacitance. The total shift in bilayer potential due to exchange of solutions is equal to the area under the current transient divided by the bilayer capacitance. In most instances the acoustic current was relatively small so that integrating the total current did not incur a significant error in estimates of ΔV.

The origin of electrostatic potentials on lipid surfaces have been the subject of many studies (reviewed by McLaughlin, 1977, 1989). Electrophoresis measurements on vesicles composed of negatively charged and zwitterionic lipids (McLaughlin et al., 1978, 1981) show that the Stern-Gouy-Chapman theory accurately predicts the electric potential at the hydrodynamic plane of shear (zeta potential). According to this theory ions can adsorb onto bilayer surfaces by binding to the lipid headgroups and so contribute to the surface charge density. The Stern equation (Eq. 2) relates the surface charge density, σ, to the lipid composition of the bilayer and the bath composition at the bilayer surface:

$$\sigma = \frac{-\{P^-\}[1 - K_2C^{2+}(0)]}{[1 + K_1C^{+}(0) + K_2C^{2+}(0)]} + \frac{2K_3\{P\}C^{2+}(0)}{[1 + K_3C^{2+}(0)]} \tag{2}$$

$$C^{2+}(0) = C^{2+} \cdot \exp\left[-2e\psi_0 \Big/ RT\right]$$

$$C^{+}(0) = C^{+} \cdot \exp\left[-e\psi_0 \Big/ RT\right]$$

where C^{2+} and C^+ (mol/m^3) are the bulk concentrations of divalent and monovalent cations, respectively, and $\{P^-\}$ and $\{P\}$ are the concentrations (mol/m^2) of negatively charged lipids (PS) and zwitterionic lipids (PC and PE), respectively. K_1 and K_2 (m^3/mol) are the intrinsic association constants for monovalent and divalent ions to PS headgroups. K_3 is the association constant for divalent cations and the headgroups of PE and PC. Mobile ions in the bath screen the bilayer surface charge and affect the surface potential, ψ_o. The Grahame equation (Eq. 3 from Grahame,

1947) relates the surface charge density to the surface potential:

$$\sigma = \pm \left\{ 2\epsilon_r \epsilon_o RT \sum_i C_i \left[\exp\left({}^{-z_1 F \psi_o}/_{RT} \right) - 1 \right] \right\}^{1/2} \quad (3)$$

The values of K_1, K_2, and K_3 have been determined previously from electrophoresis studies (McLaughlin et al., 1981). Therefore Eqs. 2 and 3 can be solved to give the bilayer surface potential under various experimental conditions. The voltage shifts, ΔV, measured from the capacitive current (see Eq. 1) are compared with the predictions of Eqs. 2 and 3 in Fig. 3. It should be stressed that these are theoretical predictions based on the above equations and do not involve any arbitrary curve fitting with adjustable parameters. It is assumed when calculating changes in surface potential during solution exchange that ΔV is due to a change in ψ_o on only the *cis* surface of the bilayer so that $\Delta V = -\psi_o$. In the cases shown in Fig. 3, $[Ca^{2+}]$ changes from 0.1 μM to a range of values up to 40 mM. The $[Ca^{2+}]$-dependent baseline changes in ΔV were measured on bilayers containing either PS or a mixture of PE, PC, and PS (see Materials and Methods) in the presence of either 250 or 500 mM CsCl in the *cis* bath.

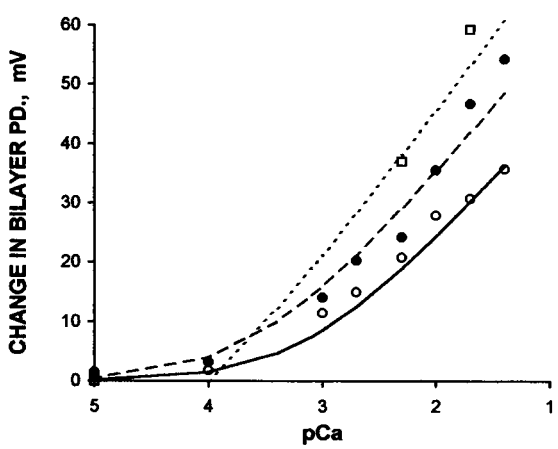

FIGURE 3 The change in the electric potential, ψ_o, of the *cis* bilayer surface (with respect to the *cis* bath) in response to a change in *cis* $[Ca^{2+}]$ shown as $\psi_{before} - \psi_{after}$. ψ_o values (*symbols*, mean of several measurements), calculated from the capacitive transients induced by several solution changes, are compared with predictions of the Stern-Gouy-Chapman theory (*lines*; Eqs. 1–3). The circles show the data obtained from bilayers composed of 30% PS, 20% PC, and 50% PE (by weight) and the squares show data from 100% PS bilayers. The $[Ca^{2+}]$ in the *cis* bath is indicated in pCa units and refers to the stating value of *cis* $[Ca^{2+}]$. *Cis* $[Ca^{2+}]$ was always changed to the same low level by flowing solutions containing 0.1 or 100 μM $[Ca^{2+}]$ past the bilayer. ●, (D14007) 30% PS, 120 pF bilayer where $[Ca^{2+}]$ was reduced to 0.1 μM in the presence of 250 mM CsCl; - - -, theory; ○, (D14358) 30% PS, 140 pF bilayer where $[Ca^{2+}]$ was reduced to 0.1 μM in the presence of 500 mM CsCl; ——, theory; □, (D16101) 100% PS, 130 pF bilayer where $[Ca^{2+}]$ was reduced to 100 μM in the presence of 500 mM CsCl; - - -, theory. The model parameters are those used by McLaughlin et al. (1981). $K_1 = 5 \times 10^{-5}$, $K_2 = 1.2 \times 10^{-2}$, $K_3 = 3 \times 10^{-3}$. Lipid concentrations $\{P^-\}$ and $\{P\}$ are calculated from the lipid weight-fraction multiplied by 2.28×10^{-6}.

Bilayer capacitive currents can be used to monitor solution exchange

The Stern-Gouy-Chapman theory accurately predicted the surface potential changes on bilayers on lipid vesicles (McLaughlin et al., 1978, 1981) and the bilayer capacitive currents observed here. We investigated the possibility of inferring the time course of the ion concentrations at the bilayer surface from the time course of the capacitive current transient. We found that knowledge of the solution composition, before and after exchange, and the bilayer capacitance provided more information than was needed to calculate the ion concentration transients from the capacitive transients using Eqs. 1–3. Therefore, we were able to predict solution transients without relying on an accurate knowledge of the bilayer capacitance. The bilayer capacitance was still used, however, to check that capacitive currents were indeed consistent with the Stern-Gouy-Chapman theory. We also took care to ensure that acoustic currents were small compared with the ion-dependent current (see above).

To test the accuracy of the capacitive current method for monitoring solution changes, we measured the time course of the capacitive current and the Cs^+ conductance of RyRs during a moderately fast decrease (5 cm H_2O puffing pressure) in $[Cs^+]$ from 500 to 100 mM (Fig. 4). The unitary current of the channel, being dependent on $[Cs^+]$, makes it a useful probe of the local $[Cs^+]$. At 40 mV, the open channel current varied linearly with *cis* $[Cs^+]$ between 100 and 500 mM. Over the same concentration range the Stern-Gouy-Chapman theory predicts that the bilayer surface potential is approximately linearly related to the log of the monovalent ion concentration. Fig. 4 *A* shows the RyR activity during a single solution exchange. The capacitive current and the decrease in channel conductance show the time interval during which the solution composition is changing near the bilayer. Fig. 4 *B* shows the time course of $[Cs^+]$ calculated from both the channel amplitude and the integral of the current transient. Both approaches gave a consistent picture of the $[Cs^+]$ time course during which $[Cs^+]$ asymptotes to a new value with an exponential time constant of 110 ms.

In many experiments the relevant solute during solution exchange is either an uncharged ligand or an ion that is present in only trace amounts. In these situations the solute of interest has no significant effect on bilayer surface potential. We tested a method for inferring concentration changes in minority compounds from associated changes in majority ions. In these experiments we predicted micromolar $[Ca^{2+}]$ from the effect of $[Cs^+]$ changes on the bilayer surface potential. RyRs are an excellent probe for testing the local $[Ca^{2+}]$ as they are opened by micromolar $[Ca^{2+}]$ and closed by millimolar $[Ca^{2+}]$ (Laver et al., 1995) and they respond in less than a millisecond to changes in $[Ca^{2+}]$ (Gyorke and Fill, 1994; Sitsapesan et al., 1995b). We find that the threshold $[Ca^{2+}]$ required for activation of skeletal and cardiac RyRs is ~0.3 μM and they are half activated by

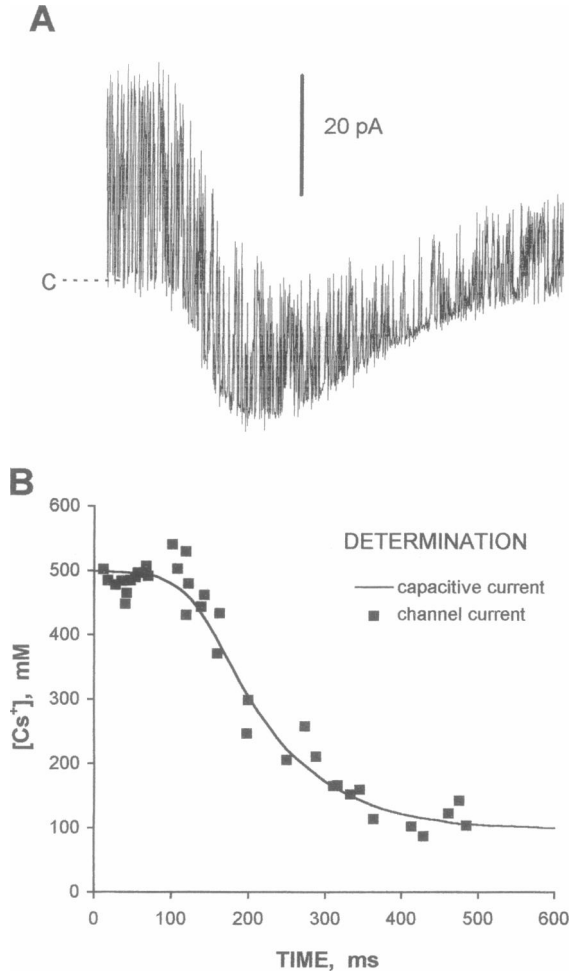

FIGURE 4 The effect of a rapid reduction of *cis* $[Cs^+]$ from 500 to 100 mM on a bilayer containing one skeletal RyR in the presence of 100 μM Ca^{2+} (D13107). The puffing solution flowed under a pressure of 5 cm H_2O. The bilayer potential was clamped at +40 mV and channel openings are seen as upward steps. The *trans* bath contained 50 mM CsCl plus 100 μM $CaCl_2$. (*A*) The dashed line labeled C indicates the level of the current baseline and the RyR closed state before the solution change. At $t = 0$ (time scale shown in *B*), the flow valve was opened. The first sign of a baseline shift (capacitive current) and the onset of solution exchange is seen at $t = 80$ ms. During the solution change, the channel current is reduced. (*B*) The time course of $[Cs^+]$ inferred from the data in *A* using two independent approaches. ■, $[Cs^+]$ predicted from the linear relationship between the RyR current at 40 mV and *cis* $[Cs^+]$ between 100 and 500 mM; ——, $[Cs^+]$ predicted from the capacitive current using the Stern-Gouy-Chapman theory (see Eqs. 1–3). The solid line approximates an exponential decay with a time constant of 110 ms.

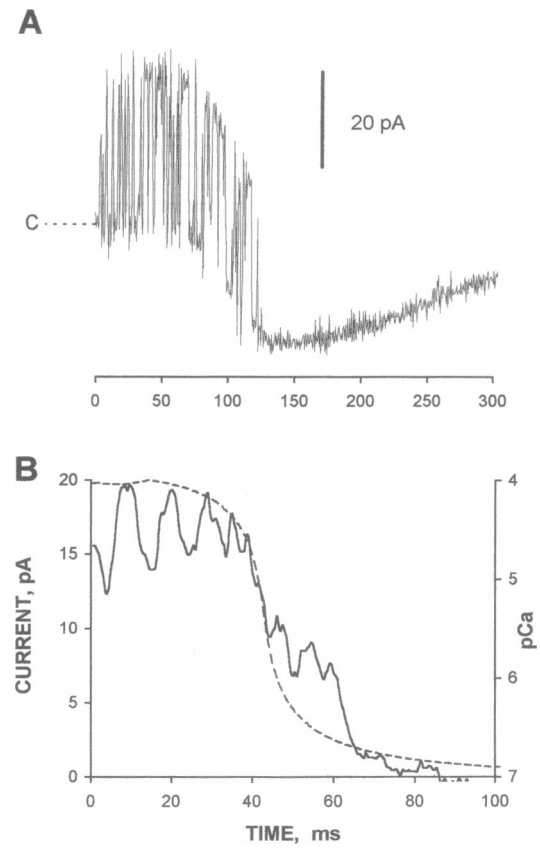

FIGURE 5 The inactivation of a skeletal RyR in response to a rapid fall in $[Ca^{2+}]$ from 100 to 0.1 μM (2 mM BAPTA plus 1 mM Ca^{2+}) by solution flow through a nozzle above the bilayer aperture using a 5-cm puffing pressure (D12506). (*A*) One episode of RyR activity. The dashed line labeled C indicates the level of the current baseline and the RyR closed state before the solution change. The flow valve was opened at $t = 0$ and the capacitive current, appearing as the baseline shift, started at $t = 50$ ms and was driven by a change in bilayer surface potential caused by the decrease in $[Cs^+]$ from 500 to 250 mM. Channel openings are indicated by upward current steps from the baseline. In this instance, the channel closed ~70 ms after the onset of solution exchange. (*B*) The average of nine episodes of RyR currents (——), stripped of the capacitive current, starting at the onset of solution exchange ($t = 0$). The time course of $[Ca^{2+}]$ (- - -), shown in pCa units, was estimated from the capacitive current as follows. $[Cs^+](t)$ at time t was calculated from the following approximate relationship consistent with Stern-Gouy-Chapman theory (see text):

$$\log([Cs^+](t)) = \log(500) - (\log(500)) - (\log(250)) \times \int_0^t I.dt \Big/ \int_0^{500ms} I.dt.$$

1 μM Ca^{2+}. The $[Ca^{2+}]$ range giving maximal opening of skeletal RyRs is 10 to 100 μM and for cardiac RyRs this range is 10 μM to 1 mM.

We measured channel activity when RyRs, open in 100 μM Ca^{2+}, were inactivated by flowing a solution containing 0.1 μM Ca^{2+} past the bilayer. Fig. 5 shows this for a single episode (Fig. 5 *A*) and for the average of nine episodes of RyR activity (Fig. 5 *B*) starting at the onset of solution exchange ($t = 0$). During solution exchange, the capacitive current (shown in Fig. 5 *A*) was driven mainly by

Total $[Ca^{2+}]$ and [BAPTA] were derived from $[Cs^+]$ by assuming equal rates of mixing of all ion species, A. Thus,

$$[A](t) = \left\{[A](t=0) \times \frac{([Cs^+] - 250)}{250}\right\} + \left\{[A](t=500) \times \frac{(500 - [Cs^+])}{250}\right\}$$

The free $[Ca^{2+}]$ was calculated from [BAPTA] and $[CaCl_2]$ (see Materials and Methods).

the change in surface potential caused by the decrease in $[Cs^+]$ from 500 to 250 mM. The $[Cs^+]$ derived from the integral of the capacitive current was used to determine total $[Ca^{2+}]$ and [BAPTA] and in turn the $[Ca^{2+}]$ transient (shown in Fig. 5 *B*). $[Ca^{2+}]$ was predicted to fall relatively quickly from 20 to 1 μM between $t = 40$ and $t = 44$ ms. In each episode, channel activity ceased (i.e., $[Ca^{2+}] \approx 0.3$ μM) at $t = 47 \pm 15$ ms ($\pm$ SD) whereas the capacitive currents predicted that $[Ca^{2+}]$ falls to 0.3 μM at $t = 54$ ms. The average current fell 50% (i.e., $[Ca^{2+}] \approx 1$ μM) at $t =$ 40 ms whereas capacitive currents predicted that this should occur at $t = 44$ ms. Clearly, $[Ca^{2+}]$ (a minority ion) can be predicted from potential changes resulting from changes in $[Cs^+]$ (the majority ion).

Modeling the time course of solution exchange

In channel records when the current baseline is obscured by channel activity or when the bilayer capacitive current is small or not simply related to bath composition, it is difficult to use the bilayer capacitive transient to monitor solution exchange. In these situations it would be better to use a model to approximate the solution exchange time course. Here we describe and evaluate a solution exchange model.

Fig. 4 shows that a few milliseconds after the onset of solution exchange the $[Cs^+]$ changes asymptotically to a new steady-state value and this could be well fitted by an exponential function (not shown). The $[Cs^+]$ time course was consistent with diffusion of ions across an unstirred layer between the bulk solution and the bilayer surface (see Discussion). More generally, the concentration of any solute, [A] at a time (t) after the onset of solution exchange is approximated by Eq. 4:

$$[A](t) = [A]_{t=\infty} \cdot \{1 - \exp(-t/\tau)\} + [A]_{t=0} \cdot \{\exp(-t/\tau)\}, \quad (4)$$

where τ is the exponential time constant of the solution exchange. The only adjustable parameter in this model is τ, which could be inferred from measurements of RyR conductance during changes in $[Cs^+]$ (e.g., Fig. 4). The mixing time for any given flow rate could be estimated from the linear relationship shown in Fig. 6. The rate of solution exchange was proportional to a flow rate of up to 30 μl/s (50 cm H_20) but leveled off at higher rates.

We assessed the accuracy of the model in predicting $[Ca^{2+}]$ transients by flowing $[Ca^{2+}]$-buffered solutions past the bilayer and comparing the model predictions with $[Ca^{2+}]$ determined by 1) bilayer capacitive transients (Fig. 7) and 2) using the Ca^{2+}-dependent activity of RyRs as a $[Ca^{2+}]$ probe (Figs. 8 and 9). Model estimates of free $[Ca^{2+}]$ were made from total $[Ca^{2+}]$ and [BAPTA], predicted by Eq. 4, using equilibrium reaction theory. The equilibrium assumption is valid as BAPTA is a rapid chelator of Ca^{2+} ($\sim 10^9$ mol/s; Stern, 1992) and the reaction kinetics are fast compared with the time for solution mixing.

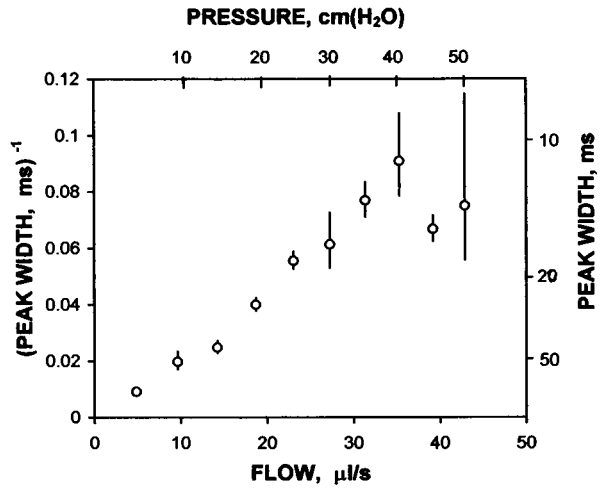

FIGURE 6 Duration of the capacitive current transient versus the flow rate and flow pressure of puffing solution (D15504). The bath solution contained 250 mM CsCl plus 5 mM $CaCl_2$. The puffing solution contained 250 mM CsCl plus 5 mM BAPTA. The width of the capacitive current transient at half-maximal amplitude was used as an indicator of the mixing time and rate of solution exchange at the bilayer surface. Error bars represent the standard deviations of three to four measurements.

$[Ca^{2+}]$ deduced from the bilayer capacitive current (Eqs. 1–3) and from the mixing model (Eq. 4) are compared in Fig. 7. Solutions containing 2 mM BAPTA were flowed onto a bilayer initially bathed in solutions containing 1–40 mM Ca^{2+}. Both approaches gave consistent results when $[Ca^{2+}]$ exceeded 1 mM. However, they deviated when $[Ca^{2+}]$ was low, when the mixing model predicted very fast decreases in $[Ca^{2+}]$. We investigated the possibility that the

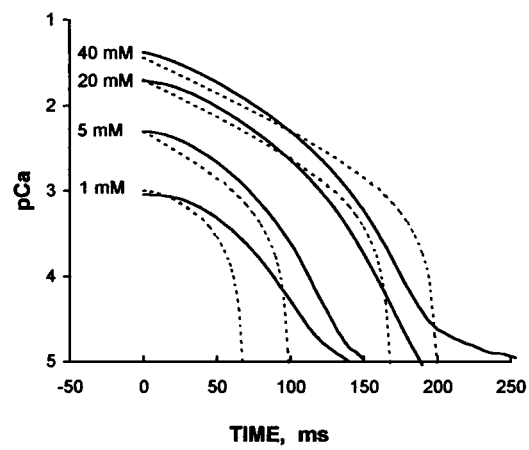

FIGURE 7 The time course of $[Ca^{2+}]$ in the *cis* compartment near a bilayer during rapid solution exchange (D14358). The *cis* bath contained 500 mM CsCl and $CaCl_2$ at the concentrations indicated at the left of each pair of traces. The bath solution was replaced by flowing a solution containing 500 mM CsCl plus 2 mM BAPTA. The solid lines show $[Ca^{2+}]$ predicted from Stern-Gouy-Chapman theoretical analysis of the capacitive current transients (Eqs. 1–3) and the dashed lines show $[Ca^{2+}]$ predicted by the mixing model (Eq. 4). The mixing time-constant that gave the closest comparison between the two approaches was 55 ms, which was used for all of the traces. The free $[Ca^{2+}]$ was calculated from [BAPTA] and $[CaCl_2]$ (see Materials and Methods).

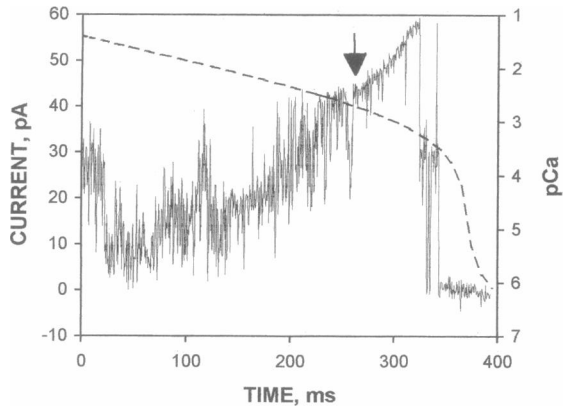

FIGURE 8 Cardiac RyR channels closing in response to a rapid fall in $[Ca^{2+}]$ from 40 mM to 0.1 μM (2 mM BAPTA plus 1 mM Ca^{2+}) by solution flow under 5 cm puffing pressure (D12528). This record (——) is one of six episodes obtained at 40 mV where solution exchange starts at $t = 0$. A large capacitive transient has been subtracted from the record. The flickery gating of the channels before $t = 200$ ms is typical of Ca^{2+} inhibition of cardiac RyRs when $[Ca^{2+}]$ exceeds 5 mM. The arrow indicates the lifting of inhibition that usually occurs when $[Ca^{2+}]$ is less than 1–2 mM. The channels close when $[Ca^{2+}]$ is lower than 0.3 μM. The dashed line shows the time course of $[Ca^{2+}]$ predicted by the mixing model (Eq. 4) using a mixing time of 110 ms.

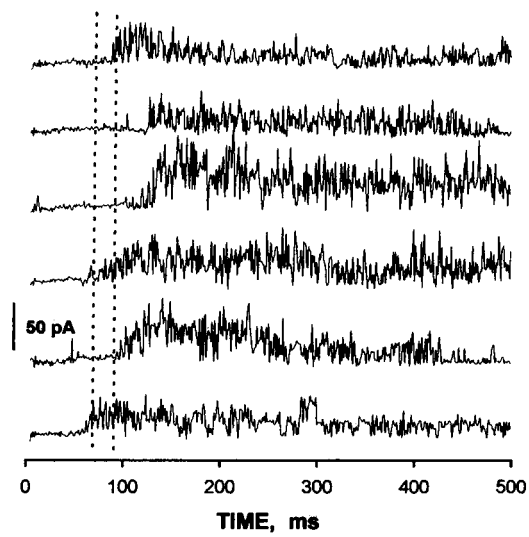

FIGURE 9 Skeletal RyR channels opening in response to a rapid rise in $[Ca^{2+}]$ from 0.1 μM (2 mM BAPTA plus 1 mM Ca^{2+}) to 200 μM (D16146). The onset of solution exchange, indicated by a small capacitive current transient, is at $t = 0$ in each record. In this instance, the capacitive current is small because the bilayer surface potential changes very little at these Ca^{2+} concentrations. The vertical dashed lines at 70 and 90 ms represent the times for $[Ca^{2+}]$ at the bilayer to reach 0.3 μM (threshold) and 10 μM (maximal open probability) predicted by the mixing model (30 cm puffing pressure giving a mixing time of 30 ms from capacitance measurements; see text). The time between the onset of solution exchange and the onset of RyR opening varied between 60 and 100 ms, and the subsequent time interval to maximal channel activity is 32 ± 6 ms, which compares favorably with the model predictions.

discrepancy may have resulted from an inability of the capacitive current to track very fast solution changes. At the start of a solution exchange the solution front (interface between the flow and bath solutions) moves across the bilayer surface. During this time the capacitive current would give an average of the nonuniform $[Ca^{2+}]$ over the bilayer surface. Thus, the capacitive current produces a $[Ca^{2+}]$ time course that is smeared compared with that encountered by each point on the bilayer. If this is the case, then $[Ca^{2+}]$ changes at a single point on the bilayer (probed by a single RyR protein) should be in better agreement with the model.

Fig. 8 shows one of six episodes from a recording of cardiac RyRs where 0.1 μM free Ca^{2+} (1 mM Ca^{2+} plus 2 mM BAPTA) plus 250 mM CsCl was flowed onto a bilayer initially in 40 mM Ca^{2+} plus 500 mM CsCl such that $\tau \approx$ 50 ms. The model predicts that, during a puff, $[Ca^{2+}]$ decreases relatively slowly to 1 mM over 300 ms and then falls very quickly from 100 to 1 μM at $t = 370$ ms (Fig. 8, dashed line). In 40 mM Ca^{2+} the channel gating is flickery as it is partially inhibited by Ca^{2+}. During solution exchange, the lifting of inhibition and increase in channel conductance gives several clues to the timing of the $[Ca^{2+}]$ decrease. The maximal RyR open probability was attained at $t = 215 \pm 27$ ms (i.e., $[Ca^{2+}] \sim 1$ mM) and the channels rapidly switch from maximally open to closed at $t = 295 \pm$ 35 ms. Given that the Ca^{2+} response of RyRs is such that they gradually activate over an order of magnitude range of $[Ca^{2+}]$ (0.3–3 μM; Chu et al., 1993), $[Ca^{2+}]$ must have fallen very rapidly at these levels. The model predicts a $[Ca^{2+}]$ time course similar to that expected from the gating behavior of the RyRs.

Fig. 9 shows the activation of RyRs by a rapid rise in $[Ca^{2+}]$ from 0.1 to 200 μM. From the puffing pressure of 30 cm H_20, it was inferred from capacity measurements (Fig. 6) that $\tau \approx 30$ ms. The mixing model predicts that *cis* $[Ca^{2+}]$ rises from inactivating levels (0.1 μM) to a threshold level (0.3 μM) in 70 ms from the onset of solution exchange. The lead time before the $[Ca^{2+}]$ rises steeply (70 ms) is long compared with τ (30 ms) because the bath solution was strongly buffered and the flow solution was unbuffered. Thus, it takes ~70 ms for BAPTA near the bilayer to dilute sufficiently to allow a substantial rise in free $[Ca^{2+}]$. We found that the time interval between the beginning of solution exchange and the onset of RyR activation varied (60 to 100 ms) between different puffs on the same channel (Fig. 9). This variation may result from the channel moving on the bilayer surface and thus sensing the solution change at different times for each puff. More importantly, the time interval between the onset of activity and maximal activity was 32 ± 6 ms, which was in reasonable agreement with the mixing model prediction of 20 ms (Eq. 4). Generally we found that the mixing model predicted the time course of $[Ca^{2+}]$ steps between a variety of levels that were consistent with the observed RyR activity during these times.

DISCUSSION

We used two methods for inferring the time course of solute concentrations at the bilayer during rapid solution exchange: 1) a capacitive current method in which the area under the bilayer capacitive current was used to calculate the shift in bilayer surface PD, which was related to ion concentrations by the Gouy-Chapman-Stern theory (Eqs. 1–3) and 2) a model for solution mixing that assumed that bath and puffing solutions exchanged exponentially (Eq. 4). These methods were in good agreement with rapid $[Cs^+]$ and $[Ca^{2+}]$ transients measured using the Cs^+-dependent conductance and Ca^{2+}-dependent gating of RyRs as a probe. Both methods gave a consistent picture of the time course of solution exchange during a puff.

The capacitive current method for measuring changes in bilayer surface potentials is a variation of a method first used by MacDonald and Bangham (1972). They found that the open-circuit potential difference across a bilayer would change when the solution in one compartment was changed. In our case the change in bilayer surface potential that measures solution change appears as a transient in the baseline current while channel gating appears as current transitions from the baseline. Another simple method for tracking rapid changes in bilayer surface potential (inner field compensation, developed by Cherny et al., 1980) is based on the dependence of the bilayer capacitance on the intramembrane PD. A sinusoidal voltage was applied to the membrane and the second harmonic of the current response indicated the presence of an intramembrane PD. Changes in the externally applied DC voltage required to null the second harmonic revealed changes in the bilayer surface PD. However, it is unlikely that ion channel recording and surface PD measurements could be done simultaneously using the inner field compensation method.

Assumptions and limitations of the capacitive current method for measuring solution changes

The capacitive current, I, will reflect 1) changes in the bilayer potential, V, and 2) changes in bilayer capacitance, C, according to Eq. 5:

$$I = C\frac{dV}{dt} + V\frac{dC}{dt}. \quad (5)$$

The integral of the current is approximated in Eq. 6:

$$\int_0^t I.dt = \bar{C}\Delta V + \bar{V}\Delta C, \quad (6)$$

where $\bar{C}$ and $\bar{V}$ are the mean values of capacitance and intramembrane PD, respectively, during the time interval of integration. In Eq. 1 we assumed that the second terms in Eqs. 5 and 6 are insignificant. However, the bilayer capacitance is known to depend on bilayer surface area, intramembrane PD (Alvarez and Latorre, 1978), and the ion composition of the bath (Ashcroft et al., 1983; Laver et al., 1984), all of which are altered by solution changes. Therefore, it is essential, when using the capacitive method for measuring solution transients, to ensure that $\bar{C}\Delta V$ is much larger than $\bar{V}\Delta C$.

Acoustic currents, caused by changes in bilayer surface area, were detected by squirting solutions at the bilayer that did not induce ionic changes (see Results). We never attempted to estimate ion transients when the acoustic current was found to be a significant fraction of the total capacitive current. The bilayer capacitance depends on the square of the bilayer PD because the bilayer is compressed by the intramembrane electric field. Bilayer capacitance increases by ~10% when a 100 mV PD is applied (see Alvarez and Latorre, 1978, and references cited therein). Bilayer capacitance also increases with ionic strength, increasing by ~10% between 1 and 100 mM (Ashcroft et al., 1983) and by an additional 3% between 100 and 1000 mM (Laver et al., 1984). A 10% change in capacitance would contribute ~10% of the capacitive current during solution exchange. An easy way to ensure that $\bar{C}\Delta V$ is much larger than $\bar{V}\Delta C$ is to see whether the capacitive current during solution exchange depends on the externally applied bilayer PD. This test is based on Eq. 5, which shows that capacitive current arising from changes in capacitance depends on the bilayer PD. We were unable to detect any dependence of capacitive transients on the externally applied bilayer PD in our experiments.

The main limitation to the temporal resolution of the capacitive current method is that different parts of the bilayer experience solution exchange at slightly different times and the current is driven by the average change in bilayer surface potential. In fact, detection of the onset of solution change at a channel protein represents the fundamental limitation to the time resolution of the flow method of solution exchange. Although the beginning of the capacitive current indicates a change of solutions at some point on the bilayer, this may not coincide with the location of the channel. To gain an estimate of the temporal resolution of the method, consider the hypothetical situation in which solution exchange occurs simultaneously over the bilayer surface. In that ideal case, the capacitive current would have a peak at the leading edge as the rate of solution change would be greatest at the beginning. In our experiments, the gradual rise in current would result from blurring of the ideal signal. The duration of the rising phase should be similar in magnitude to the temporal resolution of the technique. This was typically 50 ms when using a puffing pressure of 5 cm H_2O or 25 ms for 15 cm H_2O. Discrepancies of this magnitude can be seen in estimates of $[Ca^{2+}]$ from the mixing model and the capacitive current method in Fig. 7. The limited temporal resolution of this method would also account for inter-episode variations in the response of RyRs to changes in $[Ca^{2+}]$ as seen in Fig. 9. The resolution of this method could be improved by using bilayers with smaller diameter or by using faster solution flow rates.

Another limitation of the method is that it is restricted to situations where capacitive currents will be large enough to measure accurately. This tends to rule out situations where the membrane capacitance is small (e.g., membranes formed on fine electrodes) or where charged lipids are absent from the bilayer. In these instances, the modeling approach (method 2) could be used to predict solution transients.

Advantages of the capacitive current method for measuring solution changes

In a recent study (Sitsapesan et al., 1995a) in which bilayers were formed on the tip of a pipette, the timing of solution changes at the pipette tip was estimated from their effect on the liquid junction potential in the absence of a bilayer. The capacitive current method conveys several advantages over the junction potential method as well as the use of indicator dyes. First, solution exchange can be monitored at the same time as single-channel gating is recorded whereas before measuring the junction potentials it is necessary to rupture the membrane. Second, the size of the bilayer surface potential depends on the composition of the solution and bilayer whereas the magnitude of a liquid junction potential depends on the ion concentration gradients at the liquid interface, which are not easily determined and are difficult to control (Barry and Diamond, 1970). Third, the timing of solution changes determined by liquid junction potentials is likely to underestimate the time taken for solution exchange as junction potentials are established as soon as a liquid interface is formed at the pipette tip. However, in the presence of a bilayer membrane, the liquid interface would occur beyond the adjacent unstirred layer so that the bilayer surface would not sense the solution change until ions equilibrate within this region (Barry and Diamond, 1984). Thus, solution exchange at the bilayer surface is ultimately limited by ion diffusion in the unstirred layer whereas the formation of a liquid junction is not.

During solution exchange, the thickness of the unstirred layer, δU (microns) determines the solute equilibration rate, $t_{1/2}$ (ms) = $0.38 \times \delta^2/D$ (Diamond, 1966), and solute concentrations approach new steady-state levels at the membrane surface with a near exponential time course with $\tau = 0.5 \times \delta^2/D$. With our flow method, the fastest solution changes we could produce took 10–20 ms (Fig. 6), which indicates an unstirred region ~6 μm thick. This value is similar to estimates for the thinnest unstirred layers obtained when solutions were squirted at epithelium membranes (~10 μm, τ = 50 ms; Bindslev et al., 1974) and is considerably less than values obtained from planar membranes, in the presence of extreme, conventional stirring (25–35 μm, $\tau \approx$ 500 ms; see papers cited by Barry and Diamond, 1984).

A fourth advantage is that our method can be used to track neutral solute concentrations for which indicator dyes are not available provided the concentration of an ionic species is also altered during the solution change. And finally, the method can be used to measure changes in bilayer surface potential. As ion channels frequently exhibit voltage-dependent gating and binding kinetics with regulatory ligands, it is useful, and necessary, to be able to detect changes in bilayer potential that may be associated with changing bathing media. Quite often, the effects of possible changes in bilayer surface potential on ion channel properties are ignored. It is clear from Fig. 3 that physiologically relevant solution changes can change the bilayer surface potential and shift the bilayer potential with respect to the recording electrodes by up to 25 mV.

We wish to thank Dr. Angela Dulhunty for the hospitality of her laboratory, Heather Domaschenz for her assistance with the experiments, Ms. Lin Roden and Dr. Pauline Junankar for supplying skeletal and cardiac SR vesicles, and Professor Peter Barry for helpful discussions and critical reading the manuscript.

The work was supported by an Australian Research Council Senior Research Fellowship for D. R. Laver and a grant from the National Heart Foundation and also in part by the Illinois Affiliate of the American Heart Association for B. A. Curtis.

REFERENCES

Alvarez, O., and R. Latorre. 1978. Voltage-dependent capacitance in lipid bilayers made from monolayers. *Biophys. J.* 21:1–17.

Ashcroft, R. G., H. G. L. Coster, D. R. Laver, and J. R. Smith. 1983. The effects of cholesterol inclusion on the molecular organisation of bimolecular lipid membranes. *Biochim. Biophys. Acta.* 730:231–238.

Barry, P. H., and J. M. Diamond. 1970. Junction potentials, electrode standard potentials, and other problems in interpreting electrical properties of membranes. *J. Membr. Biol.* 3:93–122.

Barry, P. H., and J. M. Diamond. 1984. Effects of unstirred layers on membrane phenomena. *Physiol. Rev.* 64:763–871.

Bindslev, N., J. McD. Tormey, and E. M. Wright. 1974. The effects of electrical and osmotic gradients on lateral intercellular spaces and membrane conductance in a low resistance epithelium. *J. Membr. Biol.* 19:357–380.

Cherny, V. V., V. S. Sokolov, and I. G. Abidor. 1980. Determination of surface charge of bilayer lipid membranes. *Bioelectrochem. Bioenerg.* 7:413–420.

Chu, A., M. Fill, E. Stefani, and M. L. Entman. 1993. Cytoplasmic Ca^{2+} does not inhibit the cardiac muscle sarcoplasmic reticulum ryanodine receptor Ca^{2+} channel, although Ca^{2+}-induced Ca^{2+} inactivation of Ca^{2+} release is observed in native vesicles. *J. Membr. Biol.* 135:49–59.

Diamond, J. M. 1966. A rapid method for determining voltage concentration relations across membranes. *J. Physiol.* 183:83–100.

Escobar, A. L., F. Cifuentes, and J. L. Vergara. 1995. Detection of Ca^{2+}-transients elicited by flash photolysis of DM-nitrophen with a fast calcium indicator. *FEBS Lett.* 364:335–338.

Gyorke, S., and M. Fill. 1994a. Ryanodine receptor adaptation: control mechanism of Ca^{2+}-induced Ca^{2+} release in heart. *Science.* 260: 807–809.

Gyorke, S., and M. Fill. 1994b. Ca^{2+}-induced Ca^{2+} release in response to flash photolysis. *Science.* 263:967–968.

Grahame, D. C. 1947. The electrical double layer and the theory of electrocapillarity. *Chem. Rev.* 41:441–501.

Lamb, G. D., M. W. Fryer, and D. G. Stephenson. 1994. Ca^{2+}-induced Ca^{2+} release in response to flash photolysis. *Science.* 263:966.

Laver, D. R., and B. A. Curtis. 1996. Response of ryanodine receptor channels to Ca^{2+} steps produced by rapid solution exchange. *Biophys. J.* 71:732–741.

Laver, D. R., J. R. Smith, and H. G. L. Coster. 1984. The thickness of the hydrophobic and polar regions of glycerol monooleate bilayers determined from the frequency-dependence of bilayer capacitance. *Biochim. Biophys. Acta.* 772:1–9.

Laver, D. R., L. D. Roden, G. P. Ahern, K. R. Eager, P. R. Junankar, and A. F. Dulhunty. 1995. Cytoplasmic Ca^{2+} inhibits the ryanodine receptor from cardiac muscle. *J. Membr. Biol.* 147:7–22.

MacDonald, R. C., and A. D. Bangham. 1972. Comparison of double layer potentials in lipid monolayers and lipid bilayer membranes. *J. Membr. Biol.* 7:29–53.

McLaughlin, S. 1977. Electrostatic potentials at membrane-solution interfaces *Curr. Top. Membr. Trans.* 9:71–144.

McLaughlin, A., C. Grathwohl, and S. McLaughlin. 1978. The adsorption of divalent cations to phosphatidylcholine bilayer membranes. *Biochim. Biophys. Acta.* 513:338–357.

McLaughlin, S., N. Mulrine, T. Gresalfi, G. Vaio, and A. McLaughlin. 1981. Adsorption of divalent cations to bilayer membranes containing phosphatidylserine. *J. Gen. Physiol.* 77:445–473.

McLaughlin, S. 1989. The electrostatic properties of membranes *Annu. Rev. Biophys. Biophys. Chem.* 18:113–136.

Mueller, P., D. O. Rudin, H. T. Tien, and W. C. Westcott. 1962. Reconstitution of cell membrane structure in vitro and its transformation into an excitable system. *Nature.* 194:979–981.

Perrin, D. D., and I. G. Sayce. 1967. Computer calculation of equilibrium concentrations in mixtures of metal ions and complexing species. *Talanta.* 14:833–842.

Sitsapesan, R., R. A. P. Montgomery, and A. J. Williams. 1995a. A novel method for incorporation of ion channels into a planar phospholipid bilayer which allows solution changes on a millisecond timescale. *Pflugers Arch.* 430:584–589.

Sitsapesan, R., R. A. P. Montgomery, and A. J. Williams. 1995b. New insights into the gating mechanisms of cardiac ryanodine receptors revealed by rapid changes in ligand concentration. *Circ. Res.* 77: 765–772.

Stern, M. D. 1992. Buffering of calcium in the vicinity of a channel pore. *Cell Calcium* 13:183–192.

Tsien, R. Y. 1980. New calcium indicators and buffers with high selectivity against magnesium and protons: design, synthesis, and properties of prototype structures. *Biochemistry.* 19:2396–2404.

Valdivia, H. H., J. H. Kaplan, G. C. R. Ellis-Davies, and W. J Lederer. 1995. Rapid adaptation of cardiac ryanodine receptors: modulation by Mg^{2+} and phosphorylation. *Science.* 267:1997–2000.